I&EC research
Industrial & Engineering Chemistry Research

pubs.acs.org/IECR

Article

Estimating the Melting Temperatures of Type V Deep Eutectic Solvents

Gabriel Teixeira, Dinis O. Abranches, Olga Ferreira,* and João A. P. Coutinho

Cite This: https://doi.org/10.1021/acs.iecr.3c01063

Read Online

ACCESS | Metrics & More | Article Recommendations | Supporting Information

ABSTRACT: The recently proposed category of type V deep eutectic solvents (DESs), composed only of non-ionic species, has attracted great interest in the literature. However, despite their importance in solvent design, measuring the solid−liquid equilibrium (SLE) diagrams of all possible type V DES precursor combinations is unfeasible. Therefore, a reliable computational tool must be found to estimate SLE phase diagrams and, thus, the melting points of type V DESs. In this work, a total of 134 different binary eutectic systems (1744 datapoints) were gathered from the literature, and the calculation capabilities and accuracy of three different models—COSMO-RS, UNIFAC of Dortmund, and Group and Group-Interaction Contribution method (GGIC)—were evaluated. UNIFAC and COSMO-RS were, by far, the best performing models, with average absolute deviations (AADs) of, respectively, 6.9 K for 94 systems and 7.4 K for 133 systems. Due to a lack of group interaction parameters, UNIFAC could only describe 94 systems, a severe disadvantage over COSMO-RS. Moreover, despite being able to describe all 134 systems, the GGIC model resulted in an AAD of 37 K. Finally, the effect of using the different parametrizations or multiple conformers in COSMO-RS predictions was also evaluated, and the validity of neglecting heat capacity terms when performing SLE calculations was verified.

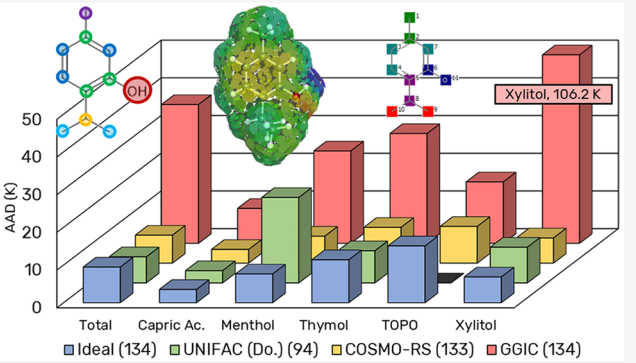

1. INTRODUCTION

Deep eutectic solvents (DESs) are green solvents reported to be a more sustainable option for a myriad of applications, including gas capture, drug delivery, synthesis, and catalysis, among others.[1−6] Unlike other types of solvents, DESs are mixtures rather than pure compounds. They are obtained by physically mixing at least two precursors, usually one hydrogen bond donor (HBD) and one hydrogen bond acceptor (HBA), leading to a significant melting temperature depression due to their strong intermolecular interactions. Thus, DESs are classified as designer solvents since their physicochemical properties can be fine-tuned for a target application by changing their precursors and relative compositions.[4,5,7,8] Because not all mixtures of organic compounds are DESs, the definition of a DES is tied to negative deviations from ideal thermodynamic behavior, which leads to lower melting temperatures than those predicted by ideal solubility curves.[6,9,10]

Due to the diversity of compounds that can be used to prepare them, DESs have been organized into five groups (I−V), depending on the nature of their precursors.[4,5] Many DESs contain at least one ionic component, but the recently proposed non-ionic type V DESs are attracting growing interest.[11] They usually have lower viscosities than their ionic counterparts, are ion- and halide-free, and can be designed to have a wider range of hydrophobicity, which is a difficult task for ionic mixtures.[10] However, the number of potential HBA/HBD combinations that can form type V DESs is overwhelming, demanding cost-intensive and time-consuming measurements to establish their solid−liquid equilibrium (SLE) phase diagrams and to know their melting points and operation range. Although predictive tools exist to estimate SLE phase diagrams, their application has been focused on types I−IV DESs,[12−17] with no extensive study reported for type V so far.

Kovács *et al.*[12] provided a broad review regarding the available modeling methods applicable to key properties of DESs such as melting point, density, viscosity, surface tension, and refractive index. The models are divided into molecular scale models, namely, density functional theory (DFT) and molecular dynamics (MD), macroscale models (COSMO-RS and PC-SAFT), and empirical (group-contribution and machine learning) methods. The authors concluded that a unified methodology is yet to be available for general and wide

Received: April 1, 2023
Revised: July 14, 2023
Accepted: July 31, 2023

application. González De Castilla *et al.*[13] also reviewed the main models applied to phase equilibria and properties of both ionic and non-ionic DES, particularly excess Gibbs energy models (g^E), equations of state (EOS), and MD simulations. The g^E-models [UNIFAC (Dortmund) or COSMO-RS] and EOS (PC-SAFT) were among the most cited and adequate for SLE calculations.

More recently, Chen *et al.*[14] combined regular solution theory and quantitative structure−activity relationship modeling aiming to predict the SLE of eutectic systems. The SLE of 99 ionic and non-ionic eutectic systems were correlated, resulting in average absolute deviations (AADs) of 13.9 K for the eutectic temperature and 0.097 (mol fraction) for the eutectic composition. The model was then used to identify 186 new potential eutectic systems, by combining the components in the database. Peng *et al.*[15] have applied the conductor-like screening model for segment activity coefficient (COSMO-SAC) to predict the SLE of 94 non-ionic and 122 ionic binary eutectic systems. According to the authors, COSMO-SAC cannot accurately account for the deviation from ideality, especially on salt-based DESs, and does not seem to improve the predictions of the non-ionic systems compared to the ideal solution model. Cappelluti *et al.*[17] combined experimental data and classical MD simulations to calculate radial distribution functions, and then predict and interpret DES formation in mixtures composed of choline chloride and phenol derivatives. Although MD is able to support the molecular level interpretation of the interactions, it is not adequate to quantitatively estimate global solid−liquid equilibria diagrams.

In this work, the modified version of UNIFAC (UNIQUAC functional group activity coefficients) of Dortmund,[18] COSMO-RS (COnductor-like Screening MOdel for Real Solvents),[19] and a Group and Group-Interaction Contribution model (GGIC)[20] were evaluated on their ability to predict the SLE of type V DES. To do so, we carried out a comprehensive comparison between these three models using a dataset of almost 1744 SLE datapoints for 134 non-ionic eutectic systems. This dataset was compiled from the literature and is summarized in Table S.1 of Supporting Information. Note that COSMO-RS and UNIFAC were chosen because of their ability to, when combined with pure-component melting properties, estimate the melting properties of mixtures without any prior knowledge of their properties. This contrasts with most equations of state, where binary parameters often need to be fitted to physicochemical properties of the mixtures. However, the requirement of prior knowledge of the melting properties (temperature, enthalpy, and/or heat capacities) of the pure compounds is a drawback, as they are sometimes unknown. Thus, this work also studies the feasibility of a GGIC model,[20] which does not require any pure-component melting property knowledge.

2. MATERIALS AND METHODS

2.1. Solid−Liquid Equilibrium. A SLE phase diagram relates the phase transitions of a mixture with the molar composition of its components. Assuming immiscible solid phases, neglecting the influence of temperature on heat capacities, and including potential solid−solid transition between T_m and T, eq 1 should be applied[21−23]

$$\ln x_i\gamma_i = \frac{\Delta_m H}{R}\left(\frac{1}{T_m} - \frac{1}{T}\right) + \frac{\Delta_m C_p}{R}\left(\frac{T_m}{T} - \ln\frac{T_m}{T} - 1\right) + \begin{cases} 0; & \text{if } T > T_{SS} \\ \dfrac{\Delta_{SS} H}{R}\left(\dfrac{1}{T_{SS}} - \dfrac{1}{T}\right); & \text{if } T \le T_{SS} \end{cases} \quad (1)$$

where γ_i is the activity coefficient of compound i at mole fraction x_i in the liquid phase, $\Delta_m H$ and T_m are the melting enthalpy and temperature of pure compound i, R is the universal gas constant, T is the absolute temperature, $\Delta_m C_p$ is the difference between the molar heat capacity of compound i in the liquid and solid phases, and $\Delta_{SS} H$ and T_{SS} are the enthalpy and temperature of the solid−solid transition of pure compound i.

Given its often negligible contribution and the scarcity of $\Delta_m C_p$ data, the second term of eq 1 is usually disregarded, resulting in eq 2, if additionally none of the pure compounds present solid−solid transitions between T_m and T

$$\ln x_i\gamma_i = \frac{\Delta_m H}{R}\left(\frac{1}{T_m} - \frac{1}{T}\right) \quad (2)$$

This approximation is particularly accepted as valid, even when $\Delta_m C_p$ data are available, if the difference between T and T_m is small.[9,24]

Nevertheless, the effects of complete eq 1 or the simpler eq 2 approximations were evaluated on this work. The corresponding ideal melting curves were calculated by setting $\gamma_i = 1$ using the melting and solid−solid transition properties listed in Table S.2. Once those equations are solved for both components of the binary mixture, the highest temperature of the two curves at any given composition is selected to draw the ideal SLE phase diagram.

2.2. COSMO-RS Model. COSMO-RS is a fully predictive tool that can estimate the chemical potential and activity coefficient of each component in a liquid mixture by combining statistical thermodynamics with quantum chemical descriptors of a molecule.[25−28] It uses DFT calculations to obtain σ-surfaces, in which the geometry of each molecule is optimized by embedding it in a continuum solvent, on top of which screened charges (σ) are calculated.[10] COSMO-RS has shown to be a robust model for the analysis of non-ionic DES,[8,29−31] being already used as a screening tool.[11]

Being an excess Gibbs energy model, COSMO-RS predicts activity coefficients in a liquid mixture as a function of composition and temperature through chemical potential calculations, as shown in eqs 3 and 4

$$\mu_i^S = \mu_i^{C,S} + \int p_i(\sigma)\cdot\mu_S(\sigma)\,\mathrm{d}\sigma \quad (3)$$

$$\ln\gamma_i = \frac{\mu_i^S(x_i) - \mu_i^p}{RT} \quad (4)$$

where μ_i^S is the partial Gibbs free energy (or chemical potential) of compound i in the system S, $\mu_i^{C,S}$ is the combinatorial contribution to the chemical potential, $p_i(\sigma)$ is unnormalized σ-profile of compound i, $\mu_S(\sigma)$ is the σ-potential of every charged surface σ in the system S, and μ_i^p is the chemical potential of the pure compound i.

These activity coefficients are combined with eqs 1 and 2 in an iterative workflow to calculate the SLE phase diagram of

https://doi.org/10.1021/acs.iecr.3c01063
Ind. Eng. Chem. Res. XXXX, XXX, XXX−XXX

each system. The melting properties of the studied compounds are listed in Table S.2. The geometry of the component and corresponding σ-surfaces were optimized in the software package TURBOMOLE V7.4 2019[32,33] using DFT with the BP-86 functional, the def_TZVP or def2_TZVPD basis sets, and the COSMO solvation model with infinite permittivity. Finally, the COSMOtherm[19] software package with the BP_TZVP_21 parametrization was used to perform all COSMO-RS-related calculations, as described in Section 3.2. In a first approach, all calculations were performed using a single conformer per molecule (usually the conformer with the lowest extent of intramolecular interactions). The same calculations were also carried out using the BP_TZVPD_FINE_21 parametrization, as compared in Section 3.2. Finally, for a few selected systems containing thymol, more than one conformer was used with the BP_TZVP_21 parametrization (Section 3.4).

2.3. Modified UNIFAC Model of Dortmund. The modified UNIFAC of Dortmund is a well-known variation of the original UNIFAC model, a group contribution excess Gibbs energy model,[34−36] that allows for the calculation of the activity coefficients (γ_i) as the sum of a combinatorial contribution related to the size and shape of the molecule, and a residual contribution containing temperature-dependent group interaction parameters,[18] as shown in eq 5

$$\ln \gamma_i = \ln \gamma_i^R + \ln \gamma_i^C \tag{5}$$

where γ_i^R and γ_i^C are, respectively, the residual and combinatorial contribution to the activity coefficient of the compound i. This predictive model was also successfully applied in the prediction of the SLE of some non-ionic DES.[31,37−40]

To estimate the melting points of the systems studied using this model, eqs 1 and 2 were solved iteratively to estimate the activity coefficients, using the modified UNIFAC of Dortmund.[18] The calculation of the activity coefficients was carried out using the software Dortmund Data Bank Predict Mix 2022.0.0.131 and the tables of parameters included there.[41] No parameters were estimated in this work.

2.4. GGIC Model. Hou *et al.*[20] proposed a group and GGIC to estimate the melting temperatures of the five types of DESs (I−V) using an extensive database of 1541 data points (996 in the training set and 545 in the testing set). This method was able to predict binary and ternary eutectic systems, showing wide applicability with an average relative deviation of 5.67% for the binary systems and of 6.13% for the ternary systems. These average relative deviations were calculated as follows

$$\mathrm{ARD}\ (\%) = \frac{100}{N}\sum_{i}^{N}\frac{|T_i^{\mathrm{cal}} - T_i^{\mathrm{exp}}|}{T_i^{\mathrm{exp}}} \tag{6}$$

where N is the total number of DES datapoints, T_i^{cal} and T_i^{exp} are the calculated and experimental temperature values, respectively. According to the model proposed by Hou *et al.*,[20] only structural fragments, group information, and the molecular weight of the components are needed to estimate SLE phase diagrams. The general equation was proposed by the authors for binary DESs

$$T_{\mathrm{m}} = A_1\left(M_{\mathrm{w}_i}{}^{\alpha}x_i\sum k_{a,i}\Delta T_{\mathrm{m}_a} + M_{\mathrm{w}_j}{}^{\alpha}x_j\sum k_{a,j}\Delta T_{\mathrm{m}_a}\right) + A_2\left(M_{\mathrm{w}_i}{}^{\alpha}x_i^2\sum k_{a,i}\Delta T_{\mathrm{m}_a} + M_{\mathrm{w}_j}{}^{\alpha}x_j^2\sum k_{a,j}\Delta T_{\mathrm{m}_a}\right) + \frac{1}{2}x_ix_jG_{\mathrm{V}} + \delta \tag{7}$$

where i and j are each component of the system, M_{w} is the molar weight of the molecule, x is the molar fraction of the component, $k_{a,b}$ is the number of times the group "a" occurs in the component b, ΔT_{m_a} is the melting temperature contribution of the group "a", A_1, A_2, α, and δ are constants, and G_{V} is the interaction factor between the components of a type V DES.

From the 996 experimental datapoints studied by Hou *et al.*,[20] only 424 datapoints (291 were correlated, and 133 predicted) corresponded to type V DES. These were included in the database studied in this work.

2.5. Deviations. The AADs between experimental and calculated melting temperatures of the system i were calculated as follows

$$\mathrm{AAD}_i\ (\mathrm{K}) = \frac{\sum |T_{\mathrm{m}}{}^{\mathrm{exp}} - T_{\mathrm{m}}{}^{\mathrm{calc}}|}{N_i} \tag{8}$$

where N_i is the total number of data points of the system i, and the subscripts "exp" and "calc" correspond to the experimental and calculated data, respectively. The AAD of each model is calculated by the average of the AAD_i of all calculated systems. Further explanation of the method used to select the calculated temperature of the models is presented in the Supporting Information and Figure S.1.

3. RESULTS AND DISCUSSION

3.1. Experimental SLE Dataset. A total of 1744 experimental melting temperature mixture data points, corresponding to 134 different non-ionic eutectic systems, were collected from the literature. The complete list is detailed in Table S.1. Information regarding the data curation can be found in Supporting Information.

To better understand the performance of the models with respect to chemical structure, the DES precursors present in the dataset described above were grouped into different categories (Table 1), loosely following the definitions proposed by Abranches and Coutinho.[10] As such, aliphatic alcohols, acids, and amines (primary and secondary) are designated as regular HBAs/HBDs (in the sense that they already establish good hydrogen bonding with themselves in their pure liquid phases). Components that only present HBA groups such as ketones, aldehydes, esters, or trioctylphosphine oxide (TOPO) are classified as lone HBAs (LHBA).

Table 1. Categories Used to Organize the DES Precursors Studied in This Work

Category	Examples
Regular HBD/regular HBA	Aliphatic alcohols, acids, and primary and secondary amines
Lone HBA	Ketones, ethers, aldehydes, and ternary amines
Asymmetric HBD	Phenols
Polyfunctional molecules	Polyols, sugars, and dicarboxylic acids
Hydrocarbons	Alkanes and aromatic compounds

https://doi.org/10.1021/acs.iecr.3c01063
Ind. Eng. Chem. Res. XXXX, XXX, XXX−XXX

Compounds where resonance strengthens and weakens, respectively, HBD and HBA sites (*e.g.*, phenolic compounds) are labeled as asymmetric HBD (AHBD). Even though thymol is a phenolic compound, it was observed that its asymmetry is partially lost in carboxylic acids systems due to their acidity;[10] therefore, to avoid another group ramification, mixtures of thymol/carboxylic acids will be categorized as regular HBAs/HBDs. Finally, hydrocarbons (no hydrogen bonding capability) and components with several functional groups were also distinguished as different categories. The latter includes polyols, sugars, dicarboxylic acids, levulinic acid, acetylsalicylic acid, ketoprofen, acetaminophen, lidocaine, 4-nitrophenol, curcumin, and hesperetin.

Given the individual compound classification provided in Table 1, the experimental SLE systems were grouped as 44 regular HBD−regular HBA systems (alcohol/alcohol, alcohol/acid, acid/acid), 8 regular HBD−lone HBA systems, 17 asymmetric HBD−regular HBA systems (thymol/aliphatic alcohol or thymol/water), 7 asymmetric HBD−lone HBA systems, 7 systems that only contain hydrocarbons (and one ether/hydrocarbon), 9 systems of hydrocarbons−HBD, and 42 systems with polyfunctional molecules. A general overview of the 134 collected systems indicates that 42 showed mostly negative deviations to the ideality, 67 systems were mostly ideal or with small deviations to ideality, and 25 presented positive deviations. Figure 1 shows the data in terms of $\ln(\gamma_{exp})$ as a function of T_{exp} for the groups mentioned earlier.

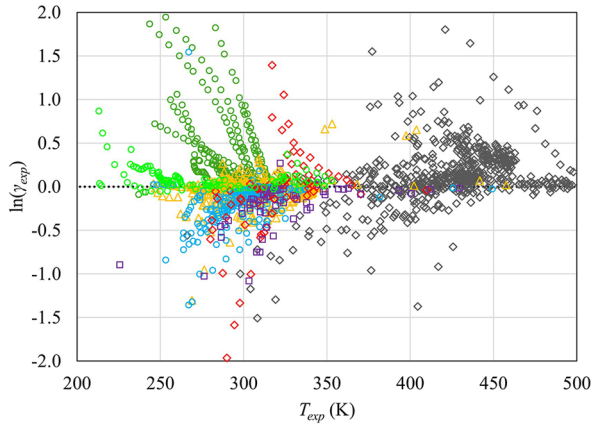

Figure 1. Experimental activity coefficients of the compounds in the liquid DES mixtures studied in this work, highlighting the thermodynamic behavior of different DES precursors. Symbols: (yellow triangle) regular HBD−regular HBA; (blue circle) asymmetric HBD−regular HBA; (red diamond) regular HBD−lone HBA; (purple square) lone HBA−asymmetric HBD; (light green circle) hydrocarbons (or hydrocarbon + ether); (dark green circle) hydrocarbon−regular HBA/HBD; (gray diamond) polyfunctional.

As expected, by mixing components of the same chemical family, the intermolecular forces in the mixtures are similar to those present in the pure components. Thus, the components display near-ideal thermodynamic behavior—$\ln(\gamma_{exp})$ close to 0. That is the case of the systems composed solely by hydrocarbons (dispersion forces) or regular HBA/HBD (alcohol + alcohol or carboxylic acid + carboxylic acid mixtures). For systems containing one hydrocarbon and one regular HBA/HBD, positive deviations are observed—$\ln(\gamma_{exp})$ larger than 0. Negative deviations are observed when stronger intermolecular forces are established in the mixture compared to those in the pure components—$\ln(\gamma_{exp})$ lower than 0. That is the case of mixtures of regular HBDs−lone HBAs or asymmetric HBDs−regular HBAs. Those deviations should be further enhanced when mixing lone HBA and asymmetric HBD. Finally, compounds with multiple functional groups present a more complex behavior as those groups can present diverse HBD/HBA sites, often resulting in close to ideal systems or positive deviations to ideality. Interestingly, systems composed of polyfunctional compounds appear as a high-melting-temperature cluster in Figure 1. Rather than being caused by mixture-related properties, this cluster is due to the already high melting temperature of the pure polyfunctional compounds studied, hinting that, to obtain mixtures liquid at room temperature, it is desirable to avoid precursors with multiple hydrogen-bonding sites.

A few examples of each category that presented the expected thermodynamic behavior are shown in Figure S.2: camphene/decane (close to ideal behavior, hydrocarbon−hydrocarbon mixture), menthol/decane (positive deviations, regular HBD/HBA−hydrocarbon mixture), menthol/ibuprofen (slight negative deviations, regular HBD−regular HBA), thymol/lauric acid (close to ideal behavior, HBD/HBA), capric acid/TOPO (negative deviations, regular HBD−lone HBA), 2,3-dimethylphenol/menthol (negative deviations, asymmetric HBD−regular HBA), thymol/camphor (strong negative deviations, asymmetric HBD−lone HBA), and sucrose/fructose (slight negative deviations, system of polyfunctional components).

Some exceptions to the expected thermodynamic behavior are shown in Figure S.3: octane/1-methylnaphtalene and menthol/flavone. In the first example, octane/1-methylnaphtalene, the positive deviations to ideality in the hydrocarbons systems are likely due to the presence of octane hindering the π interactions present in the aromatic 1-methylnaphthalene. The second example, menthol/flavone, shows how in some cases the strength of the cross-association may not be enough to result in negative deviations, as previously discussed by us.[29] This can be observed by comparing menthol/flavone (HBD/LHBA) with thymol/flavone (AHBD/LHBA). Only in the latter, higher negative deviations can be observed due to stronger cross-hydrogen bonds.

Table 2. Average Absolute Deviations of the Melting Temperatures of the Mixtures (AAD, in K) and Number of Systems Described by Each Model[a]

	Ideal solution model	GGIC	COSMO-RS (TZVP)	COSMO-RS (TZVPD-FINE)	UNIFAC (Dortmund)
Number of systems (maximum)	134	134	133	134	94
AAD (K)	9.4	36.8	7.4	7.4	6.9
Number of systems (common)			94		
AAD (K)	7.5	34.0	6.8	6.7	6.9

[a]COSMO-RS and UNIFAC were coupled to eq 2.

https://doi.org/10.1021/acs.iecr.3c01063
Ind. Eng. Chem. Res. XXXX, XXX, XXX−XXX

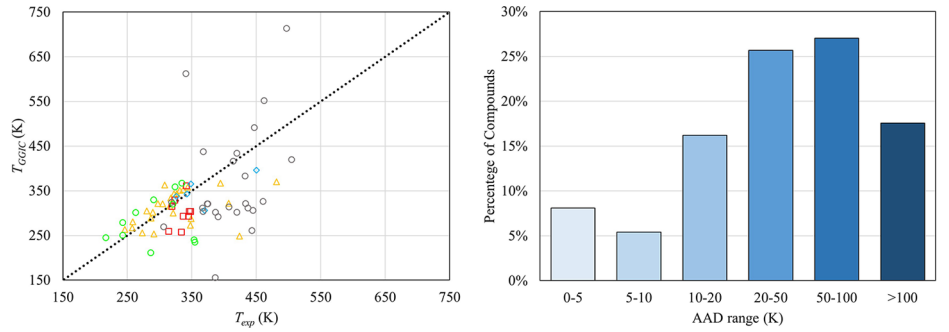

Figure 2. Experimental and estimated (by the GGIC model) melting temperature of the pure compounds (left) and the distribution of the absolute errors associated to the GGIC model predictions (right). Symbols: (yellow triangle) regular HBA or HBD; (red square) asymmetric HBD; (blue diamond) lone HBA; (light green circle) hydrocarbons; (gray circle) polyfunctional.

3.2. Models' Performance Comparison. The preliminary screening and description of eutectic systems can greatly benefit from the support of computational methods to predict the non-ideality of the systems. First, the prediction of the SLE phase diagrams was carried out considering that all studied mixtures were ideal (using eq 2, with γ_i = 1, and the melting properties collected in Table S.2). An AAD in the melting temperature of 9.4 K was obtained, as shown in Table 2, which justifies the need for the use of models capable of capturing both positive and negative deviations to ideality. In other words, it clearly justifies the use of excess Gibbs energy models (COSMO-RS and UNIFAC) that are able to estimate γ_i and, thus, eliminate the assumption of thermodynamic ideality (γ_i = 1).

Regarding model applicability, it was possible to apply the GGIC model to all SLE systems in the database (134), while COSMO-RS (TZVP parametrization) was able to describe 133 systems. The exception was the camphor/4-nitrophenol binary system for which COSMO-RS (TZVP) strongly overestimated the negative deviations to ideality, not converging to the experimental datapoint, as shown in Figure S.3. The UNIFAC (Dortmund) model had the most limited range of application, describing only 94 systems (~2/3 of the systems studied) due to the lack of group interaction parameters to represent some compounds (*e.g.*, flavone or TOPO). The AADs in the melting temperature of the mixtures were calculated for the three models and are reported in Table 2. The pure compounds' melting temperature was not included in the AAD, as it is only predicted by the GGIC model.

Hou *et al.*[20] (GGIC model) reported average relative deviations of 5.63% in the melting temperature of all the systems studied by them (1471 datapoints), including ionic and non-ionic compounds, corresponding to an AAD of 18.2 K using eq 8, which is well below the 37 K error shown in Table 2 for the non-ionic systems collected in this work. The GGIC model could satisfactorily predict most of the systems, with AAD less than 5 K on 10 systems and between 5 and 20 K on 65 systems. However, AADs higher than 50 K were obtained on 32 systems. These poor predictions are noticed specially in systems that include polyols. Examples of accurate and inaccurate predictions of the GGIC model can be found in Figures S.2 and S.3. The GGIC model parameters were fitted using all types of DES, including ionic compounds; most likely, specific parameters fitting with only type V DESs would be required to yield better results. Furthermore, the GGIC model could not accurately predict most of the melting temperatures of the pure compounds, as shown in Figure 2, with a mean absolute error of 57.9 K, which already indicates that a poor description of the complete SLE phase diagram would be obtained. An example of this type of systems is given in the SLE diagram of the mannitol/xylitol mixture shown in Figure S.3. More than half of the pure compounds (39 compounds) had an absolute error between 20 and 100 K, while only 6 compounds had an absolute error smaller than 5 K. The detailed list of compounds is presented in Table S.3.

COSMO-RS (TZVP) was able to improve the description of those systems by reducing the AAD to 6.1 K, being able to describe 75 of the 133 systems (56%) with a AAD in T_m lower than 5 K and AAD between 5 and 20 K on 48 systems (36%). Examples of COSMO-RS (TZVP) predictions can also be found in Figures S.2 and S.3. Some remarkable COSMO-RS (TZVP) prediction of complex systems can be pointed out: menthol/ibuprofen (HBD/HBA), 2,3-dimethylphenol/menthol (AHBD/HBA), thymol/camphor (AHBD/LHBA), and menthol/flavone (HBD/LHBA). On the other hand, some poor COSMO-RS (TZVP) predictions must also be pointed out: thymol/lauric acid (HBD/HBA), thymol/urea (HBD/HBA), thymol/2-phenylethanol (AHBD/HBA), and camphor/4-nitrophenol (polyfunctional mixture). In the thymol/lauric acid and thymol/2-pheylethanol systems, COSMO-RS (TZVP) predicts lower temperatures than experimentally observed ones, overestimating the negative deviations of these systems. On the other hand, positive deviations to ideality are largely overestimated in the thymol/urea system, possibly indicating the formation of two liquid phases. As such, the compositions richer in urea of the predicted solid−liquid equilibria do not have any thermodynamic significance and were excluded from the AAD calculation of all models. The same behavior can be observed on the urea/caprylic acid diagram and the same exclusion was applied. COSMO-RS (TZVP) was not able to predict the complete composition range of the SLE diagrams of camphor/4-nitrophenol and thymol/camphor. Nevertheless, it was possible to compare the model predictions with the experimental data available for the latter system.

To further understand the patterns of the COSMO-RS (TZVP) predictions, Figure S.4 shows the predicted ($T_{COSMO-RS}$) and experimental (T_{exp}) temperatures, as well as the predicted ($\gamma_{COSMO-RS}$) and experimental (γ_{exp}) activity coefficients. In the activity coefficient diagram, most of data should lie on the top right or bottom left quadrants of the diagram, meaning that at least the correct type of thermodynamic deviation (negative/positive) to ideality was estimated. Note that, in general, the expected trends discussed

https://doi.org/10.1021/acs.iecr.3c01063
Ind. Eng. Chem. Res. XXXX, XXX, XXX−XXX

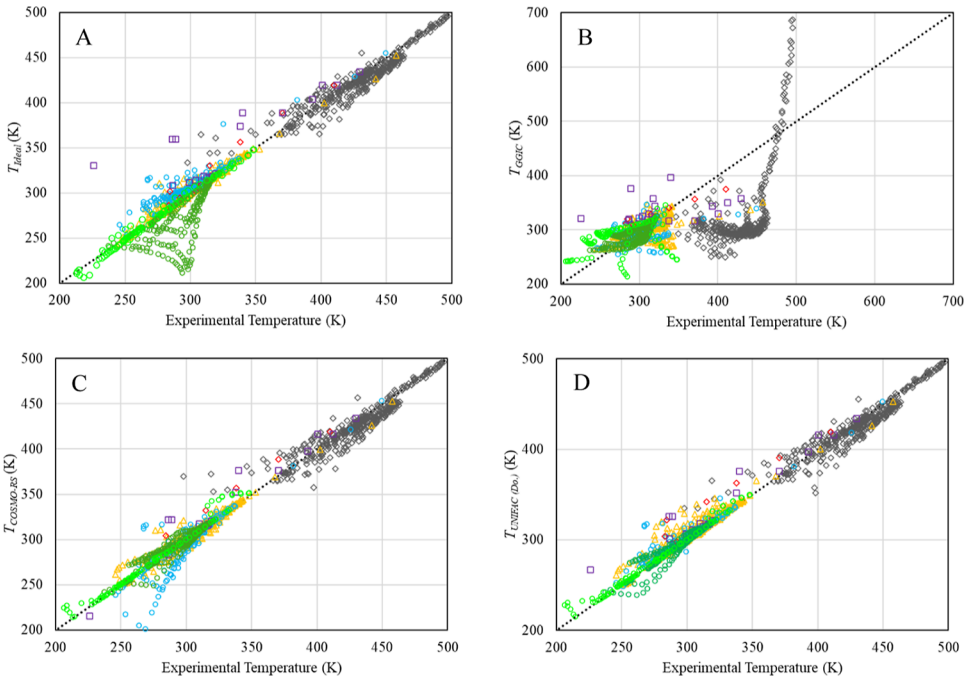

Figure 3. Correlation between experimental and estimated melting temperature of the SLE of the common 94 systems. Symbols: (yellow triangle) regular HBD−regular HBA; (blue circle) asymmetric HBD−regular HBA; (red diamond) regular HBD−lone HBA; (purple square) lone HBA−asymmetric HBD; (light green circle) hydrocarbons; (dark green circle) hydrocarbon−regular HBA/HBD mixture; (gray diamond) polyfunctional. Models used: (A) ideal model (eq 2), (B) GGIC, (C) COSMO-RS (TZVP) and (D) UNIFAC (Do.).

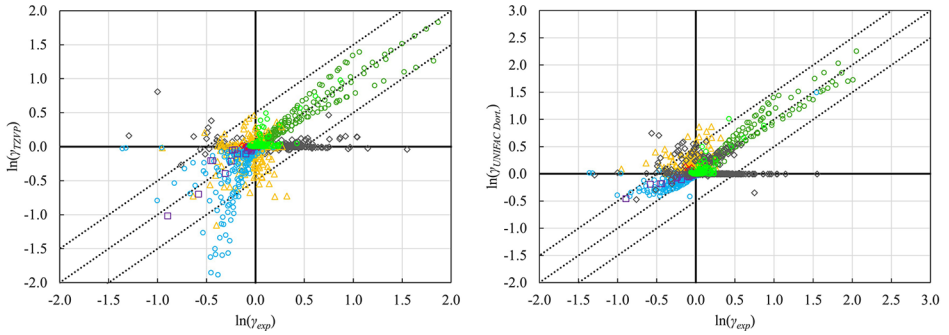

Figure 4. Correlation between experimental and estimated activity coefficients of the SLE of the common 94 systems. Model: COSMO-RS (left) and UNIFAC of Dortmund (right). Dotted lines correspond to ln $\gamma \pm 0.5$ ln unit. Symbols: (yellow triangle) regular HBD−regular HBA; (blue circle) asymmetric HBD−regular HBA; (red diamond) regular HBD−lone HBA; (purple square) lone HBA−asymmetric HBD; (light green circle) hydrocarbon mixture; (dark green circle) hydrocarbon−regular HBA/HBD mixture; (gray diamond) polyfunctional.

earlier are in line with the COSMO-RS (TZVP) predictions: most of the HBD/LHBA, AHBD/HBA, and AHBD/LHBA systems are on the bottom left quadrant ($\gamma_{\text{COSMO-RS}} < 1$, negative deviations); most of the regular HBD/HBA systems and hydrocarbon mixtures are close to the origin point of the diagram ($\gamma_{\text{COSMO-RS}} = 1$, ideal behavior); the hydrocarbon mixtures with alcohols are on the top right quadrant ($\gamma_{\text{COSMO-RS}} > 1$, positive deviations). Therefore, most of the COSMO-RS (TZVP) data show satisfactory predictions, being able to identify most of the negative and positive deviations correctly.

Regarding the modified UNIFAC of Dortmund, the SLE was only calculated for 94 systems, and for those, the lowest AAD (6.9 K) was obtained. This model was able to describe 58 of the 94 systems (62%) with a AAD smaller than 5 K, and AAD between 5 and 20 K on 29 systems (22%). Although UNIFAC showed a slightly better performance, about one-third of the initial database could not be tested. Examples of this model predictions can also be found in Figures S.2 and S.3. Similar to COSMO-RS (TZVP), UNIFAC (Do.) was able to qualitatively predict the non-ideality of most systems. The thymol/2-phenylethanol system in Figure S.3 is an example of the remarkable accuracy of this model. However, higher temperatures are predicted than the experimental data in some systems such as menthol/decane (alcohol/hydrocarbon), menthol/ibuprofen (HBD/HBA), thymol/lauric acid (HBD/HBA), 2,3-dimethylphenol/menthol (AHBD/HBA), and thymol/camphor (AHBD/LHBA) in Figure S.2, and octane/1-methylnaphthelene (hydrocarbons mixture) in Figure S.3.

To produce a fair comparison of the models, a database of the 94 systems that can be simultaneously described by all models was also compared, and the results are summarized in Table 2 and Figure 3. Interestingly, both COSMO-RS (TZVP) and UNIFAC (Dortmund) models show a similar AAD, satisfactorily predicting the set of 94 systems, with AAD of 6.8 and 6.9 K, respectively. A very high AAD is obtained by the

https://doi.org/10.1021/acs.iecr.3c01063
Ind. Eng. Chem. Res. XXXX, XXX, XXX−XXX

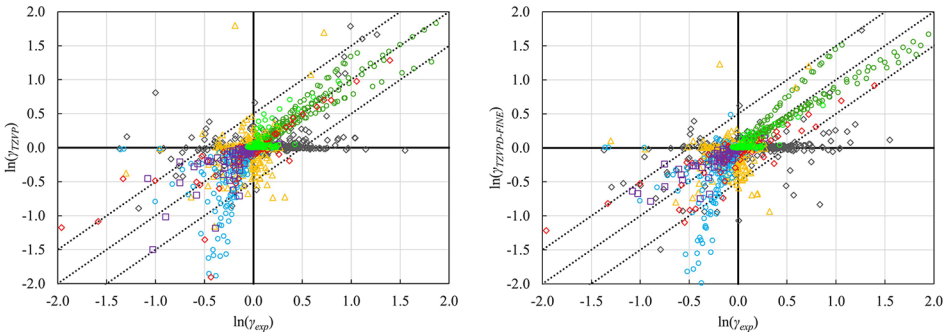

Figure 5. Correlation between experimental and estimated activity coefficients of the SLE of all systems. Model: COSMO-RS with TZVP parametrization (left) and COSMO-RS with TZVPD-FINE parametrization (right). Dotted lines correspond to the ln $\gamma \pm 0.5$ ln unit. Symbols: (yellow triangle) regular HBD−regular HBA; (blue circle) asymmetric HBD−regular HBA; (red diamond) regular HBD−lone HBA; (purple square) lone HBA−asymmetric HBD; (light green circle) hydrocarbon mixture; (dark green circle) hydrocarbon−regular HBA/HBD mixture; (gray diamond) polyfunctional.

GGIC model (34 K), with the results deteriorating at temperatures above 350 K.

To further understand the differences between the predictions of COSMO-RS (TZVP) and UNIFAC (Do.), the experimental and predicted γ of the 94 systems are plotted in Figure 4. The COSMO-RS (TZVP) predictions of all the 133 systems are also shown in Figure S.4.

It is interesting to observe how the small AAD difference between COSMO-RS (TZVP) and UNIFAC (Do.) facilitates such different activity coefficient distribution. Most datapoints in both models do not stray further from the region delimited by the dotted lines, meaning that overall satisfactory predictions are achieved. However, a few differences between the models can be noticed. Most of the regular HBD−regular HBA datapoints data are close to the origin point of the diagram on COSMO-RS (TZVP) predictions, while most UNIFAC (Do.) predictions of these systems result in positive $\ln(\gamma_{\text{UNIFAC Do.}})$ independently of the $\ln(\gamma_{\text{exp}})$. The asymmetric HBD−regular HBA systems are remarkably predicted by UNIFAC (Do.). On the other hand, COSMO-RS (TZVP) seems to overpredict the negative deviations to ideality of some AHBD/HBA systems, composed of thymol and primary alcohols.

Finally, the effect of using the TZVPD-FINE parametrization was evaluated, and the global AAD are also shown in Table 2 and Figure 5. A few examples of SLE diagrams are presented in Figure S.5.

The global AAD of TZVP and TZVPD-FINE parametrizations are very similar (7.4 K), when considering all the database, and lower than the AAD of 9.4 K of the ideal solution model. If we consider the systems with higher deviations to ideality ($\text{AAD}_{\text{ideal}} > 5$ K), a greater improvement can be seen. For these 65 systems, the TZVP parametrization improved the ideal model in 49 out of the 65 systems, decreasing the overall AAD of the latter from 15.8 to 11.3 K; while TZVPD-FINE improved 47 out of the 65 systems, decreasing the overall AAD from 15.8 to 11.2 K.

Though the global AAD are similar for both parametrization sets, some SLE diagrams are shown in Figure S.5 to exemplify that the predictions can be very different when looking at particular systems. For example, the systems menthol/salicylic acid and thymol/benzyl alcohol are better described by TZVPD-FINE than TZVP, while for menthol/hydroquinone and acetaminophen/thymol, the reverse is obtained.

There is one category (LHBA/AHBD) that includes 7 binary mixtures, in which the TZVPD-FINE parametrization greatly improves the predictions of all systems (with AAD = 5.4 K) compared to TZVP (AAD = 9.0 K) and ideal solution model (AAD = 13.7 K). That is not the case of the 17 AHBD/HBA systems, for which TZVP and TZVPD-FINE parametrizations result in similar AAD of 8.4 and 10.0 K, respectively.

3.3. Heat Capacities Difference and Solid−Solid Transitions.

To understand the impact of considering solid−solid transitions and $\Delta_{\text{m}}C_p$, the SLE of the systems in which at least one of its precursors present such properties reported in the literature were recalculated using eq 1. The $\Delta_{\text{m}}C_p$ of 21 compounds and the solid−solid transitions of 2 compounds (camphor and borneol) are shown in Table S.2, which affected 97 out of the 134 systems. COSMO-RS (TZVP) was able to predict all 97 systems while UNIFAC of Dortmund was able to predict only 73 systems. The overall results are detailed in Table 3.

Table 3. Average Absolute Deviations of the Melting Temperatures of the Mixtures (AAD, in K) and Number of Systems Described That Present Solid−Solid Transitions or $\Delta_{\text{m}}C_p$

	Ideal solution eq 1	COSMO-RS (TZVP)		UNIFAC (Dortmund)	
		Simplified eq 2	eq 1	Simplified eq 2	eq 1
Number of systems (maximum)	97	96	97	73	
AAD (K)	9.0	7.4	8.0	7.0	6.8
Number of systems (common)		73			
AAD (K)	6.9	6.7	6.9	7.0	6.8

The consideration of solid−solid transitions and $\Delta_{\text{m}}C_p$ does not have a great impact on the global AAD, which increased 0.6 K for COSMO-RS and decreased 0.2 K for UNIFAC. Nevertheless, the impact on COSMO-RS (TZVP) predictions was more significant on systems such as sucrose/fructose (AAD decreased from 8.4 to 3.3 K) or menthol/4-nitrophenol (AAD decreased from 17.3 to 11.8 K), and thymol/benzyl alcohol (AAD increased from 18.4 to 26.2 K). The inclusion of the solid−solid transition in eq 1 also allowed the prediction of

https://doi.org/10.1021/acs.iecr.3c01063
Ind. Eng. Chem. Res. XXXX, XXX, XXX−XXX

the SLE diagram of the camphor/4-nitrophenol mixture in the complete range of compositions. For UNIFAC (Do.), the largest differences in the predictions were found for the systems menthol/benzyl alcohol (AAD decreased from 6.7 to 3.6 K) and menthol/borneol (AAD increased from 6.8 to 8.9 K). The predicted SLE diagrams of these binary mixtures are shown in Figure S.6.

3.4. Impact of Conformer Choice on COSMO-RS Predictions. The effect of using multiple conformers on COSMO-RS predictions was evaluated in eight mixtures, all containing thymol (AHBD) plus a primary alcohol (HBD) as a second component (decanol, dodecanol, tetradecanol, hexadecanol, octadecanol, 2-cyclohexylethanol, benzyl alcohol or 2-phenylethanol). As previously discussed, COSMO-RS overestimated the strength of the cross-association for these systems, leading to greater negative deviations from the ideality than experimentally observed. Thus, these are the systems where the use of multiple conformers is warranted. The overestimations of these 8 systems translated to an AAD of 9.3 and 8.9 K using the TZVP and TZVPD-FINE parametrizations, respectively. Therefore, a second thymol conformer (II) was generated by rotating its hydroxyl group (the moiety expected to dominate the intermolecular interactions in these systems). The two conformers (I and II) are depicted in Figure 6 along with the results of $T_{\mathrm{COSMO\text{-}RS}}$ *versus* T_{exp} for both approaches in Figure 7. Two examples of SLE diagrams are also reported in Figure S.7.

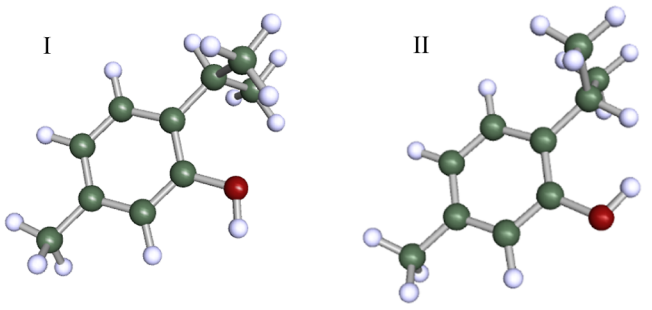

Figure 6. First (I) and second (II) thymol conformers.

The addition of a second conformer to describe thymol lowered the AAD of these eight systems from 9.4 to 2.7 K using TZVP parametrization, and the overall AAD of the 133 systems from 7.4 to 7.0 K. For consistency, the same methodology was applied to other AHBD/HBA systems, such as thymol and a secondary alcohol (borneol or menthol), which were already remarkably well predicted by COSMO-RS (TZVP) (see Figure S.5). In these cases, there was an increase in AAD from 2.3 to 3.0 K on the menthol/thymol system and from 2.5 to 4.0 K on the thymol/borneol system.

These results exemplify the impact of the selection of conformers on the predicted activity coefficients and, consequently, on the solid−liquid equilibria diagrams. The small number of systems that significantly improved their predictions with the addition of a second conformer indicates that using only one conformer per compound is already enough to yield satisfactory results, which greatly simplifies the input and effort by the user. Although more extensive testing is needed, particularly on how to consistently generate conformer sets for different molecules, the results mentioned above indicate that using more than one conformer can help to improve predictions and does not degrade them significantly when a single conformer already presented good results. The AHBD/primary alcohol case is an example of which the addition of a second AHBD conformer is desirable to obtain better predictions. Nevertheless, it still requires the user's discretion and insight to anticipate other possible complex interactions present in the systems they are screening.

4. CONCLUSIONS

This work studied the capabilities of three models (GGIC, COSMO-RS, and Dortmund's UNIFAC) to predict the SLE diagrams of an extensive number of eutectic mixtures of non-ionic compounds (1744 mixture data points from 134 binary systems), collected from the literature.

The GGIC model could be applied to all systems but had the poorest performance (AAD of 36.8 K), probably reflecting the already inaccurate description of the melting temperature of the pure components. On the other hand, both COSMO-RS (TZVP) and UNIFAC (Do.) were satisfactorily accurate on their predictions (AAD in the melting temperature of 7.4 K and 6.9 K, respectively). Though the UNIFAC method performed slightly better, it could only represent 94 systems as the lack of specific group parameters prevented the representation of more complex compounds such as flavone, lidocaine or TOPO, while COSMO-RS (TZVP) was able to represent nearly all systems, using a single conformer to describe each component as a first approach. To further evaluate COSMO-RS, binary mixtures of thymol and an alcohol were selected to study the effect of using multiple conformers. By using two conformers to describe thymol, the

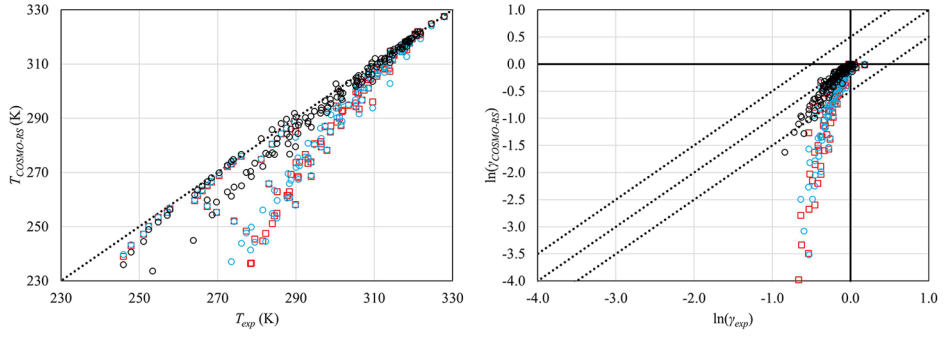

Figure 7. Comparison between the methodologies used to represent thymol in COSMO-RS for the selected systems (thymol/primary alcohol). Experimental and estimated temperatures (A) and activity coefficients (B): one conformer (I) and the TZVP parametrization (red); one conformer (I) and TZVPD-FINE (blue) and two conformers (I and II) using TZVP (black). Dotted lines (B) correspond to the ln $\gamma \pm 0.5$ ln unit.

https://doi.org/10.1021/acs.iecr.3c01063
Ind. Eng. Chem. Res. XXXX, XXX, XXX−XXX

COSMO-RS predictions of the systems thymol + primary alcohol were improved significantly, while predictions for thymol + secondary alcohol systems were not very significantly damaged. It should also be mentioned that the predictions of these activity coefficient models are dependent on the knowledge of the melting properties which are sometimes unknown or present a high uncertainty for some molecules.

Overall, weighting model performance and applicability breadth, this work demonstrates that COSMO-RS is the most effective tool to estimate the SLE phase diagrams of type V DESs. Moreover, its use can be simplified by using only a single conformer per molecule, with only a handful of exceptions. However, UNIFAC may be preferable over COSMO-RS when parameters for all functional groups of the DES precursors are available. Finally, given the poor performance of the GGIC model, there is a clear need to develop new machine learning methodologies to describe SLE phase diagrams. Such a development must be aided by a collective effort to measure and report high quality SLE data for type V DESs, particularly those mixtures that display strong negative deviations from thermodynamic ideality (mixtures containing asymmetric HBDs and lone HBAs).

■ ASSOCIATED CONTENT

Supporting Information

The Supporting Information is available free of charge at https://pubs.acs.org/doi/10.1021/acs.iecr.3c01063.

Absolute errors calculation; SLE phase diagrams of selected systems; lists of binary systems and melting properties of the pure compounds studied in this work; and distribution of the absolute errors of the pure compounds calculated by the GGIC model (PDF)

■ AUTHOR INFORMATION

Corresponding Author

Olga Ferreira − *Centro de Investigação de Montanha (CIMO) and Laboratório para a Sustentabilidade e Tecnologia em Regiões de Montanha, Instituto Politécnico de Bragança, 5300-253 Bragança, Portugal;* orcid.org/0000-0001-8414-3479; Phone: +351 273 303 087; Email: oferreira@ipb.pt

Authors

Gabriel Teixeira − *CICECO, Aveiro Institute of Materials, Complexo de Laboratórios Tecnológicos, University of Aveiro, 3810-193 Aveiro, Portugal;* orcid.org/0000-0002-5213-5359

Dinis O. Abranches − *CICECO, Aveiro Institute of Materials, Complexo de Laboratórios Tecnológicos, University of Aveiro, 3810-193 Aveiro, Portugal*

João A. P. Coutinho − *CICECO, Aveiro Institute of Materials, Complexo de Laboratórios Tecnológicos, University of Aveiro, 3810-193 Aveiro, Portugal;* orcid.org/0000-0002-3841-743X

Complete contact information is available at: https://pubs.acs.org/10.1021/acs.iecr.3c01063

Notes

The authors declare no competing financial interest.

■ ACKNOWLEDGMENTS

This work was developed within the scope of the project CICECO-Aveiro Institute of Materials, UIDB/50011/2020, UIDP/50011/2020, and LA/P/0006/2020, and CIMO-Mountain Research Center, UIDB/00690/2020 and LA/P/0007/2020, financed by national funds through the Portuguese Foundation for Science and Technology/MCTES. G.T. thanks FCT for his Ph.D. grant (UI/BD/151114/2021).

■ REFERENCES

(1) Florindo, C.; Branco, L. C.; Marrucho, I. M. Quest for Green-Solvent Design: From Hydrophilic to Hydrophobic (Deep) Eutectic Solvents. *ChemSusChem* **2019**, *12*, 1549−1559.

(2) Ali Redha, A. Review on Extraction of Phenolic Compounds from Natural Sources Using Green Deep Eutectic Solvents. *J. Agric. Food Chem.* **2021**, *69*, 878−912.

(3) Chemat, F.; Vian, M. A.; Ravi, H. K.; Khadhraoui, B.; Hilali, S.; Perino, S.; Tixier, A. S. F. Review of Alternative Solvents for Green Extraction of Food and Natural Products: Panorama, Principles, Applications and Prospects. *Molecules* **2019**, *24*, 3007.

(4) Smith, E. L.; Abbott, A. P.; Ryder, K. S. Deep Eutectic Solvents (DESs) and Their Applications. *Chem. Rev.* **2014**, *114*, 11060−11082.

(5) Hansen, B. B.; Spittle, S.; Chen, B.; Poe, D.; Zhang, Y.; Klein, J. M.; Horton, A.; Adhikari, L.; Zelovich, T.; Doherty, B. W.; Gurkan, B.; Maginn, E. J.; Ragauskas, A.; Dadmun, M.; Zawodzinski, T. A.; Baker, G. A.; Tuckerman, M. E.; Savinell, R. F.; Sangoro, J. R. Deep Eutectic Solvents: A Review of Fundamentals and Applications. *Chem. Rev.* **2021**, *121*, 1232−1285.

(6) Abranches, D. O.; Coutinho, J. A. P. Everything You Wanted to Know about Deep Eutectic Solvents but Were Afraid to Be Told. *Annu. Rev. Chem. Biomol. Eng.* **2023**, *14*, 141−163.

(7) Zdanowicz, M.; Wilpiszewska, K.; Spychaj, T. Deep Eutectic Solvents for Polysaccharides Processing. A Review. *Carbohydr. Polym.* **2018**, *200*, 361−380.

(8) Martins, M. A. R.; Silva, L. P.; Schaeffer, N.; Abranches, D. O.; Maximo, G. J.; Pinho, S. P.; Coutinho, J. A. P. Greener Terpene-Terpene Eutectic Mixtures as Hydrophobic Solvents. *ACS Sustainable Chem. Eng.* **2019**, *7*, 17414−17423.

(9) Martins, M. A. R.; Pinho, S. P.; Coutinho, J. A. P. Insights into the Nature of Eutectic and Deep Eutectic Mixtures. *J. Solution Chem.* **2018**, *48*, 962−982.

(10) Abranches, D. O.; Coutinho, J. A. P. Type V Deep Eutectic Solvents: Design and Applications. *Curr. Opin. Green Sustainable Chem.* **2022**, *35*, 100612.

(11) Abranches, D. O.; Martins, M. A. R.; Silva, L. P.; Schaeffer, N.; Pinho, S. P.; Coutinho, J. A. P. Phenolic Hydrogen Bond Donors in the Formation of Non-Ionic Deep Eutectic Solvents: The Quest for Type V DES. *Chem. Commun.* **2019**, *55*, 10253−10256.

(12) Kovács, A.; Neyts, E. C.; Cornet, I.; Wijnants, M.; Billen, P. Modeling the Physicochemical Properties of Natural Deep Eutectic Solvents. *ChemSusChem* **2020**, *13*, 3789−3804.

(13) González De Castilla, A.; Bittner, J. P.; Müller, S.; Jakobtorweihen, S.; Smirnova, I. Thermodynamic and Transport Properties Modeling of Deep Eutectic Solvents: A Review on GE-Models, Equations of State, and Molecular Dynamics. *J. Chem. Eng. Data* **2020**, *65*, 943−967.

(14) Chen, J.; Zhu, F.; Qin, H.; Song, Z.; Qi, Z.; Sundmacher, K. Rational Eutectic Solvent Design by Linking Regular Solution Theory with QSAR Modelling. *Chem. Eng. Sci.* **2022**, *262*, 118042.

(15) Peng, D.; Alhadid, A.; Minceva, M. Assessment of COSMO-SAC Predictions for Solid−Liquid Equilibrium in Binary Eutectic Systems. *Ind. Eng. Chem. Res.* **2022**, *61*, 13256−13264.

(16) Zhang, J.; Wang, R.; Zhong, Y. Identification of the Eutectic Points in the Multicomponent Systems with the High-Throughput CALPHAD Approach. *J. Phase Equilib. Diffus.* **2022**, *43*, 844−857.

(17) Cappelluti, F.; Mariani, A.; Bonomo, M.; Damin, A.; Bencivenni, L.; Passerini, S.; Carbone, M.; Gontrani, L. Stepping

Away from Serendipity in Deep Eutectic Solvent Formation: Prediction from Precursors Ratio. *J. Mol. Liq.* **2022**, *367*, 120443.
(18) Gmehling, J.; Li, J.; Schiller, M. A Modified UNIFAC Model. *Ind. Eng. Chem. Res.* **1993**, *32*, 178−193.
(19) Dassault Systèmes. *BIOVIA COSMOtherm*; Dassault Systèmes, Release 2021.
(20) Hou, X. J.; Yu, L. Y.; He, C. H.; Wu, K. J. Group and Group-Interaction Contribution Method for Estimating the Melting Temperatures of Deep Eutectic Solvents. *AIChE J.* **2022**, *68*, No. e17408.
(21) Vilas-Boas, S. M.; Cordova, I. W.; Abranches, D. O.; Coutinho, J. A. P.; Ferreira, O.; Pinho, S. P. Modeling the Solubility of Monoterpenoids with Hybrid and Predictive Thermodynamic Tools. *Ind. Eng. Chem. Res.* **2023**, *62*, 5326−5335.
(22) Choi, P. B.; Mclaughlin, E. Effect of a Phase Transition on the Solubility of a Solid. *AIChE J.* **1983**, *29*, 150−153.
(23) Weimer, R. F.; Prausnitz, J. M. Complex Formation between Carbon Tetrachloride and Aromatic Hydrocarbons. *J. Chem. Phys.* **1965**, *42*, 3643−3644.
(24) Coutinho, J. A. P.; Andersen, S. I.; Stenby, E. H. Evaluation of Activity Coefficient Models in Prediction of Alkane Solid-Liquid Equilibria. *Fluid Phase Equilib.* **1995**, *103*, 23−39.
(25) Klamt, A. Conductor-like Screening Model for Real Solvents: A New Approach to the Quantitative Calculation of Solvation Phenomena. *J. Phys. Chem.* **1995**, *99*, 2224−2235.
(26) Klamt, A.; Jonas, V.; Bürger, T.; Lohrenz, J. C. W. Refinement and Parametrization of COSMO-RS. *J. Phys. Chem. A* **1998**, *102*, 5074−5085.
(27) Eckert, F.; Klamt, A. Fast Solvent Screening via Quantum Chemistry: COSMO-RS Approach. *AIChE J.* **2002**, *48*, 369−385.
(28) Kovács, A.; Neyts, E. C.; Cornet, I.; Wijnants, M.; Billen, P. Modeling the Physicochemical Properties of Natural Deep Eutectic Solvents. *ChemSusChem* **2020**, *13*, 3789−3804.
(29) Teixeira, G.; Abranches, D. O.; Silva, L. P.; Vilas-Boas, S. M.; Pinho, S. P.; Ferreira, A. I. M. C. L.; Santos, L. M. N. B. F.; Ferreira, O.; Coutinho, J. A. P. Liquefying Flavonoids with Terpenoids through Deep Eutectic Solvent Formation. *Molecules* **2022**, *27*, 2649.
(30) Okuniewski, M.; Paduszyński, K.; Domańska, U. Phase Diagrams in Representative Terpenoid Systems: Measurements and Calculations with Leading Thermodynamic Models. *Ind. Eng. Chem. Res.* **2017**, *56*, 9753−9761.
(31) Okuniewski, M.; Paduszyński, K.; Domańska, U. Thermodynamic Study of Molecular Interactions in Eutectic Mixtures Containing Camphene. *J. Phys. Chem. B* **2016**, *120*, 12928−12936.
(32) *TURBOMOLE V7.4 2019, a Development of University of Karlsruhe and Forschungszentrum Karlsruhe GmbH, 1989−2007*; TURBOMOLE GmbH, since 2007; available from http://www.turbomole.com.
(33) Balasubramani, S. G.; Chen, G. P.; Coriani, S.; Diedenhofen, M.; Frank, M. S.; Franzke, Y. J.; Furche, F.; Grotjahn, R.; Harding, M. E.; Hättig, C.; Hellweg, A.; Helmich-Paris, B.; Holzer, C.; Huniar, U.; Kaupp, M.; Marefat Khah, A.; Karbalaei Khani, S.; Müller, T.; Mack, F.; Nguyen, B. D.; Parker, S. M.; Perlt, E.; Rappoport, D.; Reiter, K.; Roy, S.; Rückert, M.; Schmitz, G.; Sierka, M.; Tapavicza, E.; Tew, D. P.; Van Wüllen, C.; Voora, V. K.; Weigend, F.; Wodyński, A.; Yu, J. M. TURBOMOLE: Modular Program Suite for Ab Initio Quantum-Chemical and Condensed-Matter Simulations. *J. Chem. Phys.* **2020**, *152*, 184107.
(34) Weidlich, U.; Gmehling, J. A Modified UNIFAC Model. 1. Prediction of VLE, HE, and $^{3}\infty$. *Ind. Eng. Chem. Res.* **1987**, *26*, 1372−1381.
(35) Fredenslund, A.; Jones, R. L.; Prausnitz, J. M. Group-contribution Estimation of Activity Coefficients in Nonideal Liquid Mixtures. *AIChE J.* **1975**, *21*, 1086−1099.
(36) Fredenslund, A.; Gmehling, J.; Michelsen, M. L.; Rasmussen, P.; Prausnitz, J. M. Computerized Design of Multicomponent Distillation Columns Using the UNIFAC Group Contribution Method for Calculation of Activity Coefficients. *Ind. Eng. Chem. Process Des. Dev.* **1977**, *16*, 450−462.
(37) Okuniewski, M.; Paduszyński, K.; Domańska, U. (Solid + Liquid) Equilibrium Phase Diagrams in Binary Mixtures Containing Terpenes: New Experimental Data and Analysis of Several Modelling Strategies with Modified UNIFAC (Dortmund) and PC-SAFT Equation of State. *Fluid Phase Equilib.* **2016**, *422*, 66−77.
(38) Costa, M. C.; Rolemberg, M. P.; Boros, L. A. D.; Krähenbühl, M. A.; De Oliveira, M. G.; Meirelles, A. J. A. Solid-Liquid Equilibrium of Binary Fatty Acid Mixtures. *J. Chem. Eng. Data* **2007**, *52*, 30−36.
(39) Manic, M. S.; Villanueva, D.; Fornari, T.; Queimada, A. J.; MacEdo, E. A.; Najdanovic-Visak, V. Solubility of High-Value Compounds in Ethyl Lactate: Measurements and Modeling. *J. Chem. Thermodyn.* **2012**, *48*, 93−100.
(40) Domańska, U.; Marciniak, M. Experimental (Solid + Liquid) and (Liquid + Liquid) Equilibria and Excess Molar Volume of Alkanol + Acetonitrile, Propanenitrile, and Butanenitrile Mixtures. *J. Chem. Eng. Data* **2005**, *50*, 2035−2044.
(41) *DDB Predict Mix 2022.0.0.131*; DDBST GmbH: Oldenburg, Germany, 2022.

https://doi.org/10.1021/acs.iecr.3c01063
Ind. Eng. Chem. Res. XXXX, XXX, XXX−XXX